# Glacier Mass Loss Between 2010 and 2020 Dominated by Atmospheric Forcing

Geophysical Research Letters

RESEARCH LETTER
10.1029/2023GL102954

# Glacier Mass Loss Between 2010 and 2020 Dominated by Atmospheric Forcing

**Livia Jakob**[1] and **Noel Gourmelen**[1,2,3]

[1]Earthwave Ltd., Edinburgh, UK, [2]School of GeoSciences, University of Edinburgh, Edinburgh, UK, [3]IPGS UMR 7516, Université de Strasbourg, CNRS, Strasbourg, France

**Key Points:**

- Glaciers lose 2720 Gigatonnes of ice between 2010 and 2020, 2% of their total volume
- Atmospheric forcing is responsible for 89% of global glacier mass loss
- Increasing ice discharge accounts for over 50% of mass loss in the Barents and Kara seas, Patagonia, and Antarctic Periphery

**Supporting Information:**

Supporting Information may be found in the online version of this article.

**Correspondence to:**

L. Jakob,
livia@earthwave.co.uk

**Citation:**

Jakob, L., & Gourmelen, N. (2023). Glacier mass loss between 2010 and 2020 dominated by atmospheric forcing. *Geophysical Research Letters*, *50*, e2023GL102954. https://doi.org/10.1029/2023GL102954

Received 24 JAN 2023
Accepted 24 MAR 2023

**Author Contributions:**

**Conceptualization:** Livia Jakob, Noel Gourmelen
**Data curation:** Livia Jakob, Noel Gourmelen
**Formal analysis:** Livia Jakob
**Funding acquisition:** Noel Gourmelen
**Investigation:** Livia Jakob, Noel Gourmelen
**Methodology:** Livia Jakob, Noel Gourmelen
**Project Administration:** Noel Gourmelen
**Resources:** Livia Jakob, Noel Gourmelen
**Software:** Livia Jakob
**Supervision:** Noel Gourmelen
**Validation:** Livia Jakob



**Abstract** We generate a high spatial and temporal record of ice loss across glaciers globally for the first time from CryoSat-2 swath interferometric radar altimetry. We show that between 2010 and 2020, glaciers lost a total of 272 ± 11 Gt $yr^{-1}$ of ice, equivalent to a loss of 2% of their total volume during the 10-year study period. Using a simple parameterization, we demonstrate that during this period, surface mass balance anomaly dominated the mass budget, accounting for 89% ± 5% of the total ice loss. Ice discharge anomaly was responsible for 11% ± 1% of the total ice loss, and 28% ± 2% of the ice loss when excluding land-terminating sectors. Strong discharge anomaly is found over areas of changing oceanic conditions such as in the Barents and Kara Seas or in Antarctica, and areas fringed by lakes and fjords in Patagonia.

**Plain Language Summary** Glaciers outside the two ice sheets are currently the largest contributor to sea level rise. Global monitoring of these regions is a challenging task, few estimates exist and significant differences remain between these estimates. This study provides the first ever assessment of glacier mass loss globally from satellite radar altimetry, showing that glaciers have lost 2% of their volume between 2010 and 2020. In addition, for the first time, the study gives a global picture of the drivers of this glacier ice loss. The findings indicate that globally nearly 90% of all the loss in ice is due to interaction with the atmosphere, and that the ocean drives 10% of the loss. However, in regions where the ocean is changing rapidly, such as the Barents and Kara Seas or around Antarctica, ocean interaction is responsible for the majority of the ice loss.

## 1. Introduction

Glaciers distinct from the Greenland and Antarctic ice sheet are a major contributor to current sea level rise and are projected to remain so until the end of the 21st century (Rounce et al., 2023). Despite the key role glaciers play as indicators of climate change, global estimates of glacier mass loss are still limited to a handful of studies and methods due to numerous challenges in mapping glaciers and the absence of a long-term dedicated spaceborne mission for monitoring global glacier mass change (Ciracì et al., 2020; Gardner et al., 2013; Hock et al., 2019; Hugonnet et al., 2021; Slater et al., 2021; Wouters et al., 2019; Zemp et al., 2019). While at the global scale there is general agreement between methods, uncertainties remain large and significant differences exist in regional estimates and in the temporal evolution of glacier loss (Hock et al., 2019). This stems from limitations inherent to the techniques themselves, differences in spatial and temporal coverage and resolution, a relative paucity of independent estimates, and a lack of common framework between studies; global monitoring of glaciers and developing a consensus estimate therefore remains a challenging task.

The relative impact of atmospheric and oceanic warming on glacier loss is still poorly known. Recent atmospheric forcing has led to decreasing surface mass balance (SMB), mostly driven by an increase in surface melt, causing glaciers to thin (Marzeion et al., 2012). Oceanic forcing, a combination of ocean warming and submarine plumes from sub-glacial discharge (Rignot et al., 2010), results in increased frontal ablation, as well as increased ice discharge causing glaciers to dynamically thin (Cogley et al., 2011). There is still considerable uncertainty in understanding the mechanisms by which a particular forcing leads to glacier change, and in how much these various mechanisms currently contribute to glacier loss and sea level change (Tepes, Nienow, et al., 2021; Wouters et al., 2019). While the relative contribution of decreasing SMB and increasing ice discharge to sea level change is well known for the Greenland and Antarctic ice sheets (Van Den Broeke et al., 2009), the exact partitioning remains largely unknown over glaciers globally. Knowing how ice loss is partitioned between SMB and ice discharge enables process understanding on how glaciers respond to atmospheric and oceanic forcing. This knowledge is fundamental for accurate projections of glacier loss under defined climate scenarios as models

**Visualization:** Livia Jakob
**Writing – original draft:** Livia Jakob, Noel Gourmelen
**Writing – review & editing:** Livia Jakob, Noel Gourmelen

develop the ability to represent the impact of atmospheric forcing on glacier SMB and oceanic forcing on frontal ablation (Rounce et al., 2023).

## 2. Data and Methods

### 2.1. Time Dependant Glacier Elevation

Over land ice, the use of radar altimetry has traditionally been limited to ice sheets. This changed with the launch of CryoSat-2, the first altimetry mission to carry a synthetic aperture radar interferometer allowing a sharper footprint, the ability to precisely locate the position of the ground echo (Wingham et al., 2006), leading to the development and application of new algorithms (Gourmelen et al., 2018; Gray et al., 2013). Here we apply swath processing to CryoSat-2 data, which compared with the conventional Point-Of-Closest-Approach technique, increases the data volume and improves spatial as well as temporal coverage (Foresta et al., 2016, 2018; Gourmelen et al., 2018; Gray et al., 2013; Hawley et al., 2009; Jakob et al., 2021). We process *level 1b*, baseline *D* data from August 2010 to August 2020 following the approach of Gourmelen et al. (2018) (Text S1.1 in Supporting Information S1).

### 2.2. Rates of Elevation Change

Over all regions with the exception of Alaska and High Mountain Asia (HMA), we generate surface elevation changes by aggregating elevation measurements $z$ into 500 m pixels and apply a weighted (Jakob et al., 2021) plane fit approach (McMillan et al., 2014),

$$z(x, y, t) = c_0 x + c_1 y + \frac{\Delta h}{\Delta t} t + c_2, \quad (1)$$

where $x$, $y$, $t$ are easting, northing and time, respectively. The time-dependent coefficient $\Delta h/\Delta t$, is the linear rate of surface elevation change for each pixel. Over Alaska and HMA, given that data volume and coverage is lower, we apply a slightly adapted approach (Text S1.1 in Supporting Information S1).

### 2.3. Monthly and Annual Elevation and Mass Changes

In addition to linear changes, CryoSat-2's orbital sub-cycle of 30 days allows us to resolve changes at relatively high temporal resolution. Monthly elevation time-series are generated at Randolph Glacier Inventory (RGI) region and sub-region levels using a 90-day moving window. Annual changes are generated based on the monthly time series from October to September for regions in the Northern Hemisphere, from April to March for the Southern Hemisphere and from January to December for the global time series.

### 2.4. Missing Regions

Small glacier regions which are particularly challenging to capture with radar altimetry, including Western Canada and USA, Scandinavia, North Asia, Central Europe, Caucasus and Middle East, Low Latitudes and New Zealand are excluded from this analysis. They cover 3.8% of the total glacier area (RGI Consortium, 2017) and are estimated to contribute ∼5% to global mass loss of glaciers (Hugonnet et al., 2021). Our global assessment therefore applies a loss of $18.0 \pm 4.0$ Gt yr$^{-1}$ to regions not measured in this study based on estimates by Hugonnet et al. (2021) over the time span of 2010–2019, which matches up closely with the time period of this study.

### 2.5. Conversion to Volume, Mass Change, and Sea Level Contribution

We calculate volume changes using a fixed glacier area from the RGI 6.0 (RGI Consortium, 2017). As with most existing geodetic mass balance studies, we are using a fixed glacier area as defined by the RGI 6.0. We assume a standard bulk density of $\rho = 850$ kg m$^{-3}$ to convert volume changes to equivalent mass changes (Huss, 2013). Note that this assumption is considered appropriate for a wide range of conditions and longer-term trends, however, it can differ significantly for shorter term periods (Huss, 2013), which we incorporate in our uncertainties (Supplementary Text S1.3 in Supporting Information S1). To calculate the sea level equivalent we assume that all measured mass loss contributes to sea level change, and assume an area of the ocean of $3.625 \times 10^8$ km$^2$ (Cogley, 2012).

### 2.6. Partitioning SMB and Glacier Dynamics

Over marine terminating glaciers thinning can be defined as the combination of SMB and ice discharge departing from a state of balance. Disentangling the two contributions is challenging but important for mass budget and for process understanding. Over ice sheets, mass balance partitioning is usually carried out by comparing ice discharge calculated using ice velocity and ice thickness at flux gates, with SMB from regional climate models, or carried out by subtracting a SMB signal from a measurement of total mass balance obtained from either Gravity Recovery and Climate Experiment (GRACE) or geodetic methods. Both approaches require a time-period sufficiently long to include a period considered in balance (McMillan et al., 2016; Van Den Broeke et al., 2009). These observations, however, are not available with sufficient temporal coverage and accuracy over glaciers globally, hence such partitioning has only been performed over the Greenland and Antarctic ice sheet. Here we apply a variation of the approach consisting in differentiating SMB from geodetic mass balance. We define anomaly ($SMB_a$, $D_a$) as the departure from the values of SMB and discharge ($D$) for a glacier in balance displaying no change in surface elevation. Such "balance", or steady state, SMB is also sometimes referred to as climatological mean (McMillan et al., 2016). Over land-terminating sectors, glacier thinning is related to $SMB_a$ alone, while over marine-terminating sectors, glacier thinning can be related to both surface processes ($SMB_a$) and dynamic thinning related to $D_a$.

Over marine-terminating sectors in a steady state:

$$\mathrm{SMB} > 0;\ D < 0;\ \mathrm{SMB} + D = \frac{\Delta h}{\Delta t} = 0 \tag{2}$$

Over marine-terminating sectors in a state of imbalance:

$$\mathrm{SMB} + \mathrm{SMB}_a + D + D_a = \mathrm{SMB}_a + D_a = \frac{\Delta h}{\Delta t} \neq 0 \tag{3}$$

In our partitioning we seek to estimate regional $SMB_a$ and $D_a$. Note that we only consider change in ice discharge and not mass change from frontal variation, as geodetic methods are not able to resolve sub-aqueous mass loss associated with frontal migration. Our estimates therefore are relevant to mass loss impacting sea level change (Berthier et al., 2023).

To derive mass balance partitioning we expand on the approach first introduced in Tepes, Gourmelen, et al. (2021). The core idea is to derive $SMB_a$ over marine terminating glaciers by applying hypsometric averaging determined over land-terminating glaciers only. We first determine the regional height and geographical gradients of elevation change by solving for the six parameters coefficients $a_0$, $a_1$, … $a_5$ (cf. Equation 4) over land-terminating basins as defined by the RGI 6.0 (RGI Consortium, 2017), for each of the RGI regions (see Table S1 in Supporting Information S1 for coefficients):

$$\frac{\Delta h}{\Delta t} = a_0 z^3 + a_1 z^2 + a_2 z + a_3 x + a_4 y + a_5, \tag{4}$$

While hypsometry is the first order control on $SMB_a$, we find some correlation with geographical gradients hence the addition of the terms ($x$, $y$) (Table S1 in Supporting Information S1). At the regional level, this parametrization reproduces most of the observed change in elevation over land-terminating glaciers (Figure S1 in Supporting Information S1).

We then apply Equation 4 over marine-terminating sectors to estimate the region-wide $SMB_a$, which by differentiation from the measured mass balance gives us a region-wide $D_a$. A comparison with regional climate models and in-situ observations shows that this approach is able to reproduce (a) the expected $SMB_a$ over marine-terminating glaciers, (b) differences in $SMB_a$ between land- and marine-terminating sectors stemming from differences in hypsometry and spatial distribution between land and marine terminating glaciers, and (c) ice discharge for glaciers with a recorded large dynamical imbalance (Figures S2, S3, and Table S2 in Supporting Information S1).

Note that by using a glacier thinning data set we produce a direct measure of imbalance. Equivalent analysis using ice discharge requires knowledge of ice discharge of the glacier while in balance. This is an important consideration, since many marine-terminating glaciers have been in imbalance over several decades.

Further details on method, including uncertainty determination, are given as supplementary information.

10.1029/2023GL102954



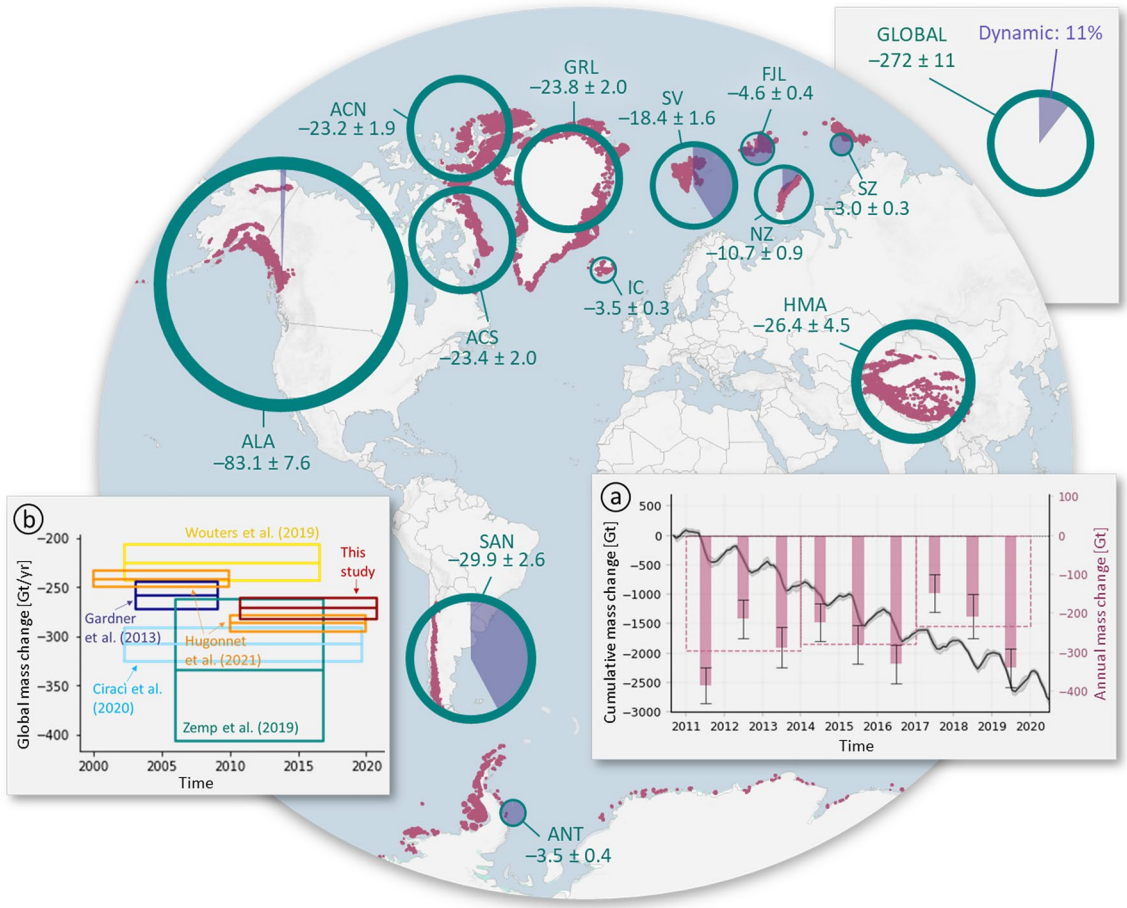


**Figure 1.** Glacier mass changes between August 2010 and August 2020. The regions displayed are Alaska (ALA), Arctic Canada North (ACN), Arctic Canada South (ACS), Greenland Periphery (GRL), Iceland (IC), Svalbard (SV), Franz-Josef-Land (FJL), Novaya Zemlya (NZ), Severnaya Zemlya (SZ), High Mountain Asia (HMA), Southern Andes (SAN) and Antarctic Periphery (ANT). The size of the circles is proportional to the mass loss, with the thickness of the line representing the uncertainty (1-sigma). The inner circle slice (purple shading) displays the proportion of mass loss due to discharge anomaly ($D_a$). The numbers display mass change in Gigatonnes per year [Gt $yr^{-1}$]. Glacier location based on the Randolph Glacier Inventory 6.0 masks are indicated in red. Graph (a) displays total cumulative monthly mass changes in Gigatonnes [Gt] (*gray line and shading*, *left y-axis*), annual mass change [Gt] (*red bars and error bars*, *right y-axis*) and 3-year averages of annual mass changes (*red dotted line, right y-axis*). Graph (b) displays various published global estimates of global mass change and their respective time spans with 1-sigma uncertainties. Our estimates for Greenland and Antarctic peripheral glaciers are added to Ciracì et al. (2020) and Wouters et al. (2019), which both do not distinguish between peripheral glaciers and ice sheet mass change.

## 3. Results and Discussion

We estimate a global mean mass loss of 272 ± 11 Gt $yr^{-1}$ (1-sigma uncertainties) between 2010 and 2020, which corresponds to a loss of 2% of global glacier ice volume (Farinotti et al., 2019) during the 10-year study period (Figure 1; Table 1). All years observed experienced ice loss, however there is considerable variation in the rates of loss from year to year. For example, the years 2011 (385 ± 46 Gt $yr^{-1}$) and 2019 (340 ± 50 Gt $yr^{-1}$), both years with exceptional arctic summer melt, experienced the largest losses, while 2017 (148 ± 49 Gt $yr^{-1}$) experienced the lowest loss (Figure 1a). Between 2010 and 2020, glaciers have contributed 0.75 ± 0.03 mm $yr^{-1}$ to sea level rise, equivalent to the loss of both ice sheets combined over the same period (Velicogna et al., 2020), and equivalent to about 25% of global sea-level budget (Nerem et al., 2018).

Alaska is the highest contributor to global mass change from glaciers with a mass balance of −83.1 ± 7.6 Gt $yr^{-1}$, which equates to a loss of just over 5% of its total ice volume (Farinotti et al., 2019) during the 10-year study period. Both the northern and southern regions of the Canadian Arctic, showed extensive mass losses; 23.3 ± 1.9 Gt $yr^{-1}$ in Arctic Canada North (ACN) and 23.4 ± 2.0 Gt $yr^{-1}$ in Arctic Canada South. We observe a total mass loss of 23.8 ± 2.0 Gt $yr^{-1}$ from peripheral glaciers in Greenland with most sectors having experienced mass loss. Temporally resolved changes also highlight large losses in 2011 (68 ± 5 Gt) and 2012 (66 ± 5 Gt) followed by 6 years of

**Table 1**
*Regional Breakdown of Global Mass Change Between 2010 and 2020*

| Region | Area [km$^2$] | Mass change [Gt yr$^{-1}$] | Mass change [m w.e. yr$^{-1}$] | SLE 2010–2020 [mm] | Volume loss 2010–2020 [%] | Area land-terminating [%] | SMB$_a$ [Gt yr$^{-1}$] | $D_a$ [Gt yr$^{-1}$] |
|---|---|---|---|---|---|---|---|---|
| 1 Alaska | 86,700 | −83.1 ± 7.6 | −0.96 ± 0.09 | 2.29 ± 0.21 | 5.2 | 67.3 | −83.0 ± 7.6 | −0.1 ± 0.0 |
| 3 Arctic Canada North | 105,100 | −23.2 ± 1.9 | −0.22 ± 0.02 | 0.64 ± 0.05 | 1.0 | 53.3 | −23.9 ± 1.9 | +0.7 ± 0.1 |
| 4 Arctic Canada South | 40,900 | −23.4 ± 2.0 | −0.57 ± 0.05 | 0.65 ± 0.06 | 3.2 | 92.6 | −23.6 ± 2.0 | +0.2 ± 0.0 |
| 5 Greenland periphery | 89,700 | −23.8 ± 2.0 | −0.27 ± 0.02 | 0.66 ± 0.06 | 1.8 | 65.3 | −25.9 ± 2.0 | +2.1 ± 0.2 |
| 6 Iceland | 11,100 | −3.5 ± 0.3 | −0.32 ± 0.03 | 0.10 ± 0.01 | 1.1 | 100.0 | −3.5 ± 0.3 | – |
| 7 Svalbard | 34,000 | −18.4 ± 1.6 | −0.54 ± 0.05 | 0.51 ± 0.04 | 2.9 | 56.1 | −11.4 ± 0.9 | −7.0 ± 0.7 |
| 8 Russian Arctic | 51,600 | −18.4 ± 1.0 | −0.36 ± 0.02 | 0.51 ± 0.03 | 1.5 | 35.2 | −10.5 ± 0.9 | −7.9 ± 0.4 |
| 8(a) Novaya Zemlya | 22,100 | −10.7 ± 0.9 | −0.49 ± 0.04 | 0.30 ± 0.03 | – | 38.1 | −9.5 ± 0.8 | −1.2 ± 0.1 |
| 8(b) Franz-Josef-Land | 12,800 | −4.6 ± 0.4 | −0.36 ± 0.03 | 0.13 ± 0.01 | – | 9.7 | −1.1 ± 0.1 | −3.5 ± 0.3 |
| 8(c) Severnaya Zemlya | 16,700 | −3.0 ± 0.3 | −0.18 ± 0.02 | 0.08 ± 0.01 | – | 50.9 | +0.1 ± 0.3 | −3.1 ± 0.3 |
| 13–15 High Mountain Asia | 97,600 | −26.4 ± 4.5 | −0.27 ± 0.05 | 0.73 ± 0.12 | 4.4 | 100.0 | −26.4 ± 4.5 | – |
| 17 Southern Andes | 29,400 | −29.9 ± 2.6 | −1.02 ± 0.09 | 0.83 ± 0.07 | 6.6 | 41.6 | −16.6 ± 1.3 | −13.3 ± 1.3 |
| 19 Antarctic periphery | 132,900 | −3.5 ± 0.4 | −0.03 ± 0.00 | 0.10 ± 0.01 | 0.1 | 1.0 | +0.1 ± 2.1 | −3.6 ± 0.4 |
| Total (CryoSat-2 measured) | 679,000 | −253.6 ± 10.1 | −0.37 ± 0.01 | 7.00 ± 0.28 | 1.9 | 54.5 | −224.7 ± 9.9 | −28.9 ± 1.6 |
| Remaining regions (not CryoSat-2 measured) | 26,800 | −18.0 ± 4.0 | −0.67 ± 0.15 | 0.50 ± 0.11 | 11.4 | 100.0 | −18.0 ± 4.0 | – |
| Total, excluding Greenland and Antarctic | 483,200 | −244.3 ± 10.6 | −0.51 ± 0.02 | 6.74 ± 0.30 | 3.0 | 69.8 | −216.9 ± 10.2 | −27.4 ± 1.6 |
| Global | 705,800 | −271.6 ± 10.8 | −0.39 ± 0.02 | 7.49 ± 0.30 | 2.0 | 56.3 | −242.7 ± 10.1 | −28.9 ± 1.5 |

*Note.* We display mass change [Gt yr$^{-1}$], specific mass balance [m w.e. yr$^{-1}$], sea level equivalent (SLE) [mm per decade], proportion of land-terminating sectors and partitioning between Surface Mass Balance anomaly (SMB$_a$) and discharge anomaly ($D_a$) of the mass imbalance. Ice volume loss percentages are calculated using the regional glacier volume by Farinotti et al. (2019). Regions not measured by swath data include Western Canada and USA, Scandinavia, North Asia, Central Europe, Caucasus and Middle East, Low Latitudes and New Zealand, and are provided using the results of Hugonnet et al. (2021) over the time span 2010 to 2019.

relatively lower mass loss (Figure 2), a pattern also observed over the Greenland Ice Sheet during the same period (The IMBIE Team, 2019). The year 2019 marked a return to high loss (46 ± 5 Gt) coinciding with an exceptionally high melt year (Sasgen et al., 2020). Icelandic ice caps have experienced a mass loss of 3.5 ± 0.6 Gt yr$^{-1}$ between 2010 and 2020 with high interannual variability and lower mass loss in the middle of the decade as previously noted (Foresta et al., 2016; Hock et al., 2019; Wouters et al., 2019). Thinning in Svalbard is amongst the highest observed (Figure S4 in Supporting Information S1), with a specific mass loss of 0.54 ± 0.05 m w.e. yr$^{-1}$ (−18.4 ± 1.6 Gt yr$^{-1}$). Particularly noticeable events are the exceptional melt season in 2013 and the surge of Basin-3 over Austfonna initiated in 2012 (Dunse et al., 2015; Lang et al., 2015; McMillan et al., 2014). The Russian Arctic has lost 18.4 ± 1.0 Gt yr$^{-1}$ of ice between 2010 and 2020. The highest mass loss has occurred in Novaya Zemlya (NZ) (10.7 ± 0.9 Gt yr$^{-1}$), followed by Franz-Josef-Land (4.6 ± 0.4 Gt yr$^{-1}$) and Severnaya Zemlya (SZ) (3.0 ± 0.3 Gt yr$^{-1}$), with large interannual variabilities for all sub-regions. The conditions leading to high summer melt in Svalbard in 2013 also appear to impact NZ and Franz-Josef-Land with high rate of ice loss. In contrast, SZ appears to be under a different forcing regime, with large mass losses in 2011 and post-2015. High Mountain Asia has lost over 4% of its total ice volume during the 10-year study period and is a region that exhibits one of the largest mass losses, with 26.4 ± 4.5 Gt yr$^{-1}$. In the southern hemisphere, the fastest thinning is seen in the Southern Andes (SAN), with a specific mass loss of 1.02 ± 0.09 m w.e. yr$^{-1}$ (29.9 ± 2.6 Gt yr$^{-1}$), of which 90% is occurring on the Patagonian Ice Fields (26.9 ± 2.2 Gt yr$^{-1}$). For Antarctic peripheral glaciers, and despite covering the largest glacier area (RGI Consortium, 2017), mass loss was moderate at 3.5 ± 0.3 Gt yr$^{-1}$. Most of the mass loss was recorded on the Antarctica Peninsula (2.5 ± 0.2 Gt yr$^{-1}$ on the Western Peninsula; 0.9 ± 0.1 Gt yr$^{-1}$ on the North-East Peninsula) and Marie Byrd Land (3.2 ± 0.2 Gt yr$^{-1}$), and most of the mass gain in the Bellingshausen Sea sector (1.6 ± 0.2 Gt yr$^{-1}$) and the Alexander Island (1.8 ± 0.2 Gt yr$^{-1}$). Rates of ice loss of Antarctic peripheral glaciers show considerable variation during the studied period with relatively lower loss between 2014 and 2017 (Figure 2), a pattern that is also observed over the ice sheet (Velicogna et al., 2020).

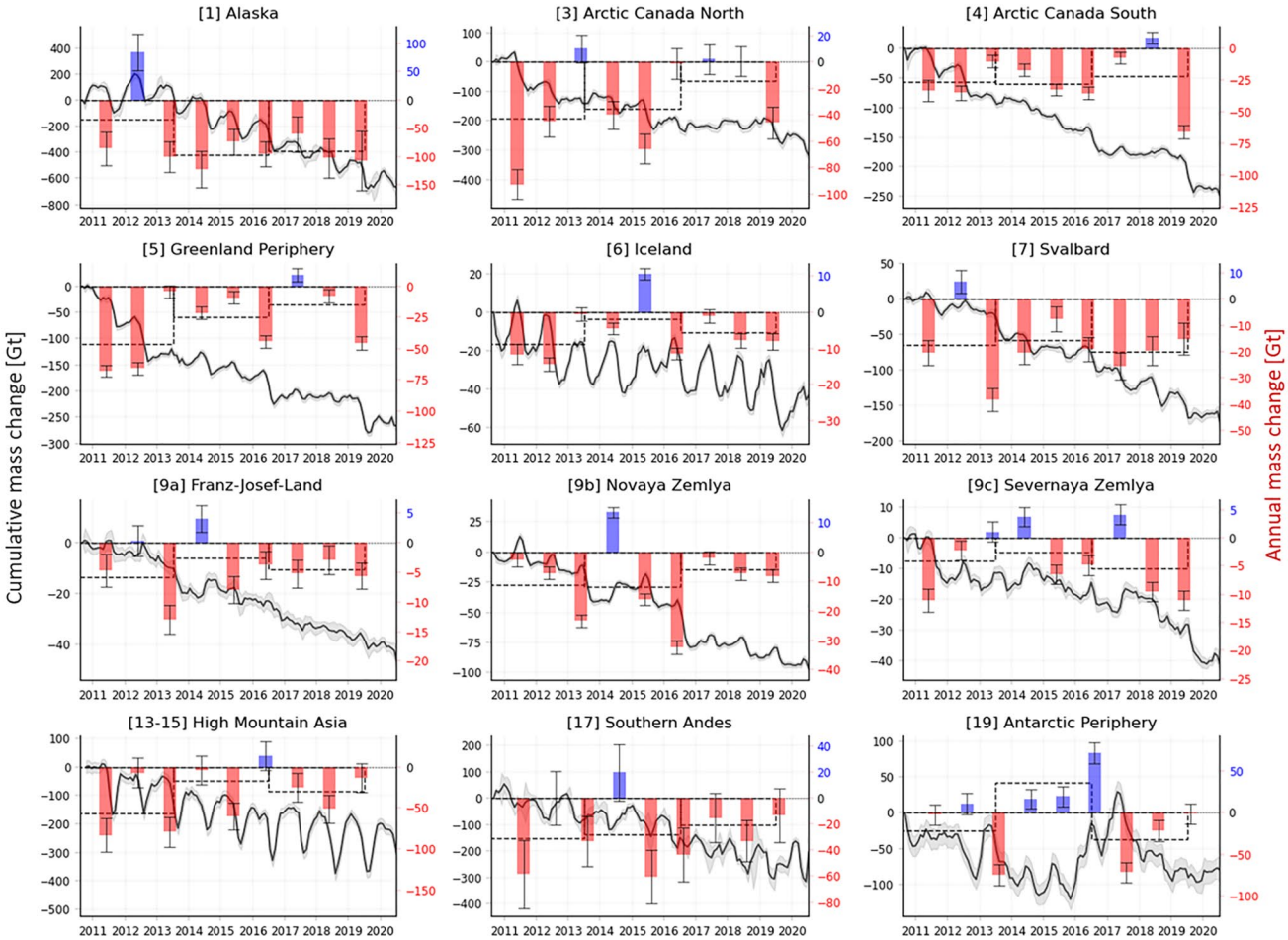


**Figure 2.** Time-dependent glacier mass changes for each Randolph Glacier Inventory glacier region. The gray line (*left axis*) displays cumulative monthly mass change in Gigatonnes [Gt] with confidence interval. The bars (*right axis*) display annual mass change in Gigatonnes [Gt] with error bars (1-sigma), with the blue shading representing mass gain and the red shading representing mass loss. The dotted bars are 3-year averages of annual mass changes.

### 3.1. Comparison With Other Mass Balance Estimates

While there is some degree of variability in the various global estimates reflecting differences in study time-span, potential measurement error and biases (Figure 1b), our global estimate is consistent with other global studies (Ciracì et al., 2020; Gardner et al., 2013; Hugonnet et al., 2021; Wouters et al., 2019; Zemp et al., 2019). Comparisons at the regional scale is also generally consistent with earlier studies but with some notable differences (Ciracì et al., 2020; Hugonnet et al., 2021; Wouters et al., 2019) (Figure S5 in Supporting Information S1).

The spatial and temporal overlap with two direct measures of time-dependent mass changes by GRACE (Ciracì et al., 2020; Wouters et al., 2019) allows an assessment of the impact of measurement uncertainties and constant density assumption on our short term mass balance estimates. The latter is a somewhat simplified but needed assumption given the lack of auxiliary information over glaciers, ignoring variabilities in density over shorter time periods (Huss, 2013). We generally find a strong correlation between our annual, 3-year, and 6-year mass change assessment and the two GRACE studies with no significant bias (Figures S6, S7, S8, and S9 in Supporting Information S1). We also find that the differences between our study and the GRACE studies are of a similar magnitude as the differences between the two GRACE studies, indicating that at regional scale, the choice in the processing steps for GRACE can lead to differences of similar magnitudes as those stemming from differences between geodetic and gravimetry-based methods.

A closer look at interannual variability shows a good agreement in both timing and amplitude with GRACE time-series, with well documented events such as the relatively low mass change in Alaska between 2010 and

2013, or in Iceland between 2013 and 2015 due to recent large winter accumulation (Foresta et al., 2016), the rapid mass loss associated with the 2012 Basin-3 surge and the 2013 summer melt in Svalbard, or the exceptional 2013 and 2016 summer melt in NZ (Ciracì et al., 2018) (Figures S7 and S8 in Supporting Information S1). A more recent estimate using high-resolution digital elevation model (DEM) differencing (Hugonnet et al., 2021) appears less sensitive to interannual variability, producing notable differences in the Arctic and in the Antarctic Periphery regions as seen in the cumulative mass loss time series (Figures S7 and S8 in Supporting Information S1). As described in Hugonnet et al. (2021), interannual variability is not captured by the related method because of the relatively lower temporal coverage of the DEM differencing study with an average of 39 observations between the period of 2000 and 2019. A spatial comparison in Iceland with Hugonnet et al. (2021) over a matching time period displays elevation change differences around the ice cap margins, where our coverage is usually lower and where interpolation is needed, showing the superior ability of high-resolution DEMs to resolve these local rates of change (Figure S10 in Supporting Information S1). However, differences at the ice cap margin cover a relatively small area, hence the impact of the elevation change differences on the total volume change is relatively low, indeed, most of the volume change difference is found between around 1,000 and 1,500 m elevation. Similar observations are made over for example, NZ or ACN (Figure S10 in Supporting Information S1) although varying signs of the differences are found. We note that both the amplitude and the signs of the differences correlate with the rapid mass change events highlighted by both, CryoSat-2 and GRACE. For example, CryoSat-2 shows lower spatial rates of change relative to Hugonnet et al. (2021) in Iceland during the period when higher accumulation occurs, but higher spatial rates of change in NZ during the period when higher surface melt occurs. Although we cannot rule out sources of uncertainty in both data sets, it suggests that a substantial proportion of the spatial differences between this study and the DEM differencing study are related to the relatively lower sensitivity of the DEM differencing study to short-term mass change variability.

Despite broad agreement within uncertainty, the spatial and temporal comparison of mass balance estimates reveals differences between studies using different sensors and techniques, and even between studies relying on a similar sensor. A community-based, multi-sensor comparison and synthesis exercise (The IMBIE Team, 2018, 2019) would provide an opportunity to understand these differences better and reduce sources of uncertainty in global glacier change. Such a study would also improve process understanding by exploiting differences between methods related to real geophysical processes.

### 3.2. Glacier Surface Mass Balance and Ice Discharge

Land-terminating glaciers account for 56% of glacier area and for 65% of the global glaciers mass loss, while marine terminating glaciers account for 35% of global glacier mass loss with contribution from both, enhanced ice discharged and decreasing SMB. By partitioning mass loss we find that globally atmospheric forcing is the dominant process leading to glacier loss, with $SMB_a$ accounting for 89% ± 5% of glaciers volume loss, whilst discharge anomaly accounts for 11% ± 1% (Figure 1). When excluding land-terminating sectors, $D_a$ accounts for a significant portion of volume loss (28% ± 2%) (Table S3 in Supporting Information S1), comparable to that observed over the Greenland Ice Sheet (Mouginot et al., 2019). There is however considerable variation between regions and when accounting for the relative frequency of marine-terminating and land-terminating glaciers. Overall, mass loss in Alaska, Arctic Canada, and Greenland periphery is largely due to surface processes during the study time period. This is consistent with recent findings showing that glacier discharge has been relatively stable, or decreased slightly, over the last 2 decades (Kochtitzky et al., 2022). This is in contrast to the Barents and Kara sea regions fringing Svalbard and the Russian arctic. On SZ, mass imbalance is entirely driven by $D_a$, while $D_a$ accounts for 77% ± 9% and 38% ± 5% of total loss for Franz-Josef-Land and Svalbard respectively. When only considering Svalbard's marine-terminating sectors, more than half of the loss is of dynamic origin owing to recent speedup of several marine-terminating glaciers (McMillan et al., 2014; Strozzi et al., 2017). In the nearby NZ, $D_a$ is more moderate, accounting for 11% ± 1% of imbalance, 18% ± 2% if only considering marine-terminating sectors. We note that for some of these dynamically active sectors, increase in ice discharge can be associated with frontal advance, hence geodetic mass balance reflects sea level contribution while actual glacier mass loss may be less. Dynamic thinning from glaciers on the Patagonian Ice fields such as Jorge Montt, Videma, Upsala, Grey, and Tyndall are a large contributor to mass loss, whilst we observe mass gain for the Pio Xi glacier. Overall $D_a$ accounts for a significant proportion of volume loss in the SAN, 45% ± 6% if all glaciers are considered and 61% ± 8% when excluding land-terminating sectors. Specifically, $D_a$ is equal to $-3.1 \pm 0.3$ Gt $yr^{-1}$ in marine-terminating sectors and to $-10.2 \pm 0.9$ Gt $yr^{-1}$ in lake-terminating sectors (Table S4 in Supporting

Information S1). Finally, over Antarctic peripheral glaciers $D_a$ appears to be the sole cause of ice loss as the SMB is generally near-balance. This observation is consistent with observations that ice sheet wide SMB trend has been generally constant over the last 40 years, where loss is the result of discharge anomalies in several large marine sectors (The IMBIE Team, 2018). Whilst we observe ice loss of dynamic origin in marine-terminating sectors, shelf-terminating glaciers tend to show little signs of dynamic loss, potentially pointing to the role of ice shelf buttressing in modulating the impact of climate on land ice (Table S4 in Supporting Information S1).

These regions of elevated $D_a$ are associated with significant shift in oceanic conditions, such as the Atlantification of the Barents and Kara sea sector (Tepes, Nienow, et al., 2021), or with the ubiquity of proglacial lakes and fjords in Patagonia enhancing mass loss (Sutherland et al., 2020).

## 4. Conclusions

Here we present a high spatial and temporal resolution data set of global glacier mass imbalance between August 2010 and August 2020 from CryoSat-2 swath altimetry (Gourmelen et al., 2018). We provide spatially and temporally resolved monthly, annual, 3- and 10-yearly averaged estimates of mass changes between 2010 and 2020 for all larger glacier regions defined in the RGI (RGI Consortium, 2017), the missing RGI regions account for 3.8% of global glacier area. We then use a novel altimetry-based approach to model change in glacier elevation resulting from SMB anomaly and provide the first global estimate of the partition of mass loss between SMB anomaly ($SMB_a$) and ice discharge anomaly ($D_a$). We show that SMB is the main source of mass imbalance globally, but that $D_a$ is non negligible and plays a key role in specific regions undergoing change in oceanic conditions, or where glaciers terminates in lakes and fjords.

This first global and time-dependent estimate of glacier volume and mass change from radar altimetry, is a new independent data set for monitoring glacier change, and is unique in terms of its combination of high spatial and temporal sampling, contributing to the expanding toolbox of glacier mass balance measurements. In the future, combining these multiple geodetic, gravimetric, and in-situ observations, coupled with growing modeling capabilities, should lead to an increased accuracy in global glacier health assessment, improve understanding of the underlying processes linking glacier loss with climate forcings, as well as improve our ability to project future glacier change.

One such insight is the prevalence of SMB driven loss overall, but also that $D_a$ drives a significant amount of glacier loss globally and plays a major role in key sectors. This highlights the importance of ocean thermal forcing and increasing ice discharge in current glacier loss and its potential in driving rapid and large future loss as the climate warms. This and future improvements in mass balance partitioning should help process understanding as well as support the development of current models in representing glacier behavior under atmospheric and oceanic forcing, resulting in better and more reliable projections of future glacier freshwater production and sea level contribution (Rounce et al., 2023).

## Data Availability Statement

Glacier mass changes presented in this work can be accessed at https://doi.org/10.5281/zenodo.7565993 and https://doi.org/10.5281/zenodo.7740808. CryoSat-2 swath data are available through the CryoTEMPO EOLIS product at https://cryotempo-eolis.org/product-overview/ (last access: March 2023) and via the cs2eo data platform at cs2eo.org (last access: March 2023). Raw CryoSat-2 data are available via the European Space Agency at https://earth.esa.int/eogateway/missions/cryosat/data (last access: March 2023). ArcticDEM and REMA are available at the Polar Geospatial Center: https://www.pgc.umn.edu/data (last access: March 2023). TanDEM-X DEMs are available at the German Space Agency https://download.geoservice.dlr.de/TDM90 (last access: March 2023). RGI glacier masks and attributes are available at the National Snow and Ice Data Center: https://nsidc.org/data/nsidc-0770/versions/6 (last access: March 2023). In-situ glacier mass balance are available at the World Glacier Monitoring Service: https://wgms.ch/data-exploration/ (last access: March 2023).

**Acknowledgments**
This work was performed under the European Space Agency's Support to Science Element CryoSat + Mountain Glacier project (4000114224/15/I-SBo) and raw swath data are provided under the European Space Agency's CryoTEM-PO-EOLIS project (4000128095/19/I-DT). We particularly wish to thank Mark Drinkwater, Diego Fernandez and Stephen Plummer at the ESA for actively supporting the development of CryoSat-2 beyond the initial primary objectives of the mission. We are thankful to Johanna Kauffert for preparing reference DEMs and her input on gap filling methods for surging glaciers. We are grateful to Alex Horton, Martin Ewart, Sophie Dubber and Carolyn Michael for their inputs on optimizing the data processing and pipeline. We wish to thank Bert Wouters and an anonymous reviewer for providing constructive comments during the review process. We further thank the ESA for providing free access to CryoSat-2 data, the Randolph Glacier Inventory (RGI) consortium for providing free access to glacier masks, the German Aerospace Center (DLR) for providing free access to the TanDEM-X DEM, and the Polar Geospatial Center (PGC) for providing free access to the ArcticDEM and REMA.

## References

Berthier, E., Floricioiu, D., Gardner, A. S., Gourmelen, N., Jakob, L., Paul, F., et al. (2023). Measuring glacier mass changes from space—A review. *Reports on Progress in Physics*, *86*(3), 036801. https://doi.org/10.1088/1361-6633/acaf8e

Ciracì, E., Velicogna, I., & Sutterley, T. (2018). Mass balance of Novaya Zemlya Archipelago, Russian high arctic, using time-variable gravity from GRACE and altimetry data from ICESat and CryoSat-2. *Remote Sensing*, *10*(11), 1817. https://doi.org/10.3390/rs10111817

Ciracì, E., Velicogna, I., & Swenson, S. (2020). Continuity of the mass loss of the world's glaciers and ice caps from the GRACE and GRACE Follow-On missions. *Geophysical Research Letters*, *47*(9). https://doi.org/10.1029/2019GL086926

Cogley, J. G. (2012). Area of the ocean. *Marine Geodesy*, *35*(4), 379–388. https://doi.org/10.1080/01490419.2012.709476

Cogley, J. G., Hock, R., Rasmussen, L., Arendt, A., Bauder, A., Braithwaite, R., et al. (2011). Glossary of glacier mass balance and related terms. https://doi.org/10.5167/uzh-53475

Dunse, T., Schellenberger, T., Hagen, J. O., Kääb, A., Schuler, T. V., & Reijmer, C. H. (2015). Glacier-surge mechanisms promoted by a hydro-thermodynamic feedback to summer melt. *The Cryosphere*, *9*(1), 197–215. https://doi.org/10.5194/tc-9-197-2015

Farinotti, D., Huss, M., Fürst, J. J., Landmann, J., Machguth, H., Maussion, F., & Pandit, A. (2019). A consensus estimate for the ice thickness distribution of all glaciers on Earth. *Nature Geoscience*, *12*(3), 168–173. https://doi.org/10.1038/s41561-019-0300-3

Foresta, L., Gourmelen, N., Pálsson, F., Nienow, P., Björnsson, H., & Shepherd, A. (2016). Surface elevation change and mass balance of Icelandic ice caps derived from swath mode CryoSat-2 altimetry. *Geophysical Research Letters*, *43*(23), 12138–12145. https://doi.org/10.1002/2016GL071485

Foresta, L., Gourmelen, N., Weissgerber, F., Nienow, P., Williams, J. J., Shepherd, A., et al. (2018). Heterogeneous and rapid ice loss over the Patagonian Ice Fields revealed by CryoSat-2 swath radar altimetry. *Remote Sensing of Environment*, *211*, 441–455. https://doi.org/10.1016/j.rse.2018.03.041

Gardner, A. S., Moholdt, G., Cogley, J. G., Wouters, B., Arendt, A. A., Wahr, J., et al. (2013). A reconciled estimate of glacier contributions to sea level rise: 2003 to 2009. *Science*, *340*(6134), 852–857. https://doi.org/10.1126/science.1234532

Gourmelen, N., Escorihuela, M., Shepherd, A., Foresta, L., Muir, A., Garcia-Mondejar, A., et al. (2018). CryoSat-2 swath interferometric altimetry for mapping ice elevation and elevation change. *Advances in Space Research*, *62*(6), 1226–1242. https://doi.org/10.1016/j.asr.2017.11.014

Gray, L., Burgess, D., Copland, L., Cullen, R., Galin, N., Hawley, R., & Helm, V. (2013). Interferometric swath processing of Cryosat data for glacial ice topography. *The Cryosphere*, *7*(6), 1857–1867. https://doi.org/10.5194/tc-7-1857-2013

Hawley, R. L., Shepherd, A., Cullen, R., Helm, V., & Wingham, D. J. (2009). Ice-sheet elevations from across-track processing of airborne interferometric radar altimetry. *Geophysical Research Letters*, *36*(22), L22501. https://doi.org/10.1029/2009GL040416

Hock, R., Rasul, G., Adler, C., Gruber, B., Hirabayashi, Y., Jackson, M., et al. (2019). High mountain areas. In H.-O. Pörtner, D. C. Roberts, V. Masson-Delmotte, P. Zhai, M. Tignor, E. Poloczanska, et al. (Eds.), *IPCC special report on the ocean and cryosphere in a changing climate*.

Hugonnet, R., McNabb, R., Berthier, E., Menounos, B., Nuth, C., Girod, L., et al. (2021). Accelerated global glacier mass loss in the early twenty-first century. *Nature*, *592*(7856), 726–731. https://doi.org/10.1038/s41586-021-03436-z

Huss, M. (2013). Density assumptions for converting geodetic glacier volume change to mass change. *The Cryosphere*, *7*(3), 877–887. https://doi.org/10.5194/tc-7-877-2013

Jakob, L., Gourmelen, N., Ewart, M., & Plummer, S. (2021). Spatially and temporally resolved ice loss in High Mountain Asia and the Gulf of Alaska observed by CryoSat-2 swath altimetry between 2010 and 2019. *The Cryosphere*, *15*(4), 1845–1862. https://doi.org/10.5194/tc-15-1845-2021

Kochtitzky, W., Copland, L., Van Wychen, W., Hugonnet, R., Hock, R., Dowdeswell, J. A., et al. (2022). The unquantified mass loss of Northern Hemisphere marine-terminating glaciers from 2000–2020. *Nature Communications*, *13*(1), 5835. https://doi.org/10.1038/s41467-022-33231-x

Lang, C., Fettweis, X., & Erpicum, M. (2015). Stable climate and surface mass balance in Svalbard over 1979–2013 despite the Arctic warming. *The Cryosphere*, *9*(1), 83–101. https://doi.org/10.5194/tc-9-83-2015

Marzeion, B., Jarosch, A. H., & Hofer, M. (2012). Past and future sea-level change from the surface mass balance of glaciers. *The Cryosphere*, *6*(6), 1295–1322. https://doi.org/10.5194/tc-6-1295-2012

McMillan, M., Leeson, A., Shepherd, A., Briggs, K., Armitage, T. W. K., Hogg, A., et al. (2016). A high-resolution record of Greenland mass balance. *Geophysical Research Letters*, *43*(13), 7002–7010. https://doi.org/10.1002/2016GL069666

McMillan, M., Shepherd, A., Gourmelen, N., Dehecq, A., Leeson, A., Ridout, A., et al. (2014). Rapid dynamic activation of a marine-based Arctic ice cap. *Geophysical Research Letters*, *41*(24), 8902–8909. https://doi.org/10.1002/2014GL062255

Mouginot, J., Rignot, E., Bjørk, A. A., van den Broeke, M., Millan, R., Morlighem, M., et al. (2019). Forty-six years of Greenland Ice Sheet mass balance from 1972 to 2018. *Proceedings of the National Academy of Sciences*, *116*(19), 9239–9244. https://doi.org/10.1073/pnas.1904242116

Nerem, R. S., Beckley, B. D., Fasullo, J. T., Hamlington, B. D., Masters, D., & Mitchum, G. T. (2018). Climate-change–driven accelerated sea-level rise detected in the altimeter era. *Proceedings of the National Academy of Sciences*, *115*(9), 2022–2025. https://doi.org/10.1073/pnas.1717312115

RGI Consortium. (2017). *Randolph glacier inventory—a dataset of global glacier outlines: Version 6.0*. (Technical report). Global Land Ice Measurements from Space. Retrieved from https://www.glims.org/RGI/00_rgi60_TechnicalNote.pdf

Rignot, E., Koppes, M., & Velicogna, I. (2010). Rapid submarine melting of the calving faces of West Greenland glaciers. *Nature Geoscience*, *3*(3), 187–191. https://doi.org/10.1038/ngeo765

Rounce, D. R., Hock, R., Maussion, F., Hugonnet, R., Kochtitzky, W., Huss, M., et al. (2023). Global glacier change in the 21st century: Every increase in temperature matters. *Science*, *379*(6627), 78–83. https://doi.org/10.1126/science.abo1324

Sasgen, I., Wouters, B., Gardner, A. S., King, M. D., Tedesco, M., Landerer, F. W., et al. (2020). Return to rapid ice loss in Greenland and record loss in 2019 detected by the GRACE-FO satellites. *Communications Earth & Environment*, *1*(1), 8. https://doi.org/10.1038/s43247-020-0010-1

Slater, T., Lawrence, I. R., Otosaka, I. N., Shepherd, A., Gourmelen, N., Jakob, L., et al. (2021). Review article: Earth's ice imbalance. *The Cryosphere*, *15*(1), 233–246. https://doi.org/10.5194/tc-15-233-2021

Strozzi, T., Kääb, A., & Schellenberger, T. (2017). Frontal destabilization of Stonebreen, Edgeøya, Svalbard. *The Cryosphere*, *11*(1), 553–566. https://doi.org/10.5194/tc-11-553-2017

Sutherland, J. L., Carrivick, J. L., Gandy, N., Shulmeister, J., Quincey, D. J., & Cornford, S. L. (2020). Proglacial lakes control glacier geometry and behavior during recession. *Geophysical Research Letters*, *47*(19), e2020GL088865. https://doi.org/10.1029/2020GL088865

Tepes, P., Gourmelen, N., Nienow, P., Tsamados, A., Shepherd, A., & Weissgerber, F. (2021). Changes in elevation and mass of Arctic glaciers and ice caps, 2010–2017. *Remote Sensing of Environment*, *261*, 112–481. https://doi.org/10.1016/j.rse.2021.112481

Tepes, P., Nienow, P., & Gourmelen, N. (2021). Accelerating ice mass loss across arctic Russia in response to atmospheric warming, sea ice decline, and Atlantification of the Eurasian Arctic Shelf Seas. *Journal of Geophysical Research: Earth Surface*, *126*(7), e2021JF006068. https://doi.org/10.1029/2021jf006068

The IMBIE Team. (2018). Mass balance of the Antarctic Ice Sheet from 1992 to 2017. *Nature*, *558*(7709), 219–222. https://doi.org/10.1038/s41586-018-0179-y

The IMBIE Team. (2019). Mass balance of the Greenland Ice Sheet from 1992 to 2018. *Nature*, *579*(7798), 233–239. https://doi.org/10.1038/s41586-019-1855-2

Van Den Broeke, M., Bamber, J., Ettema, J., Rignot, E., Schrama, E., van de Berg, W. J., et al. (2009). Partitioning recent Greenland mass loss. *Science*. https://doi.org/10.1126/science.1178176

Velicogna, I., Mohajerani, Y., A, G., Landerer, F., Mouginot, J., Noel, B., et al. (2020). Continuity of ice sheet mass loss in Greenland and Antarctica from the GRACE and GRACE Follow-On missions. *Geophysical Research Letters*, *47*(8), L11501. https://doi.org/10.1029/2020GL087291

Wingham, D., Francis, C. R., Baker, S., Bouzinac, C., Brockley, D., Cullen, R., et al. (2006). CryoSat: A mission to determine the fluctuations in Earth's land and marine ice fields. *Advances in Space Research*, *37*(4), 841–871. https://doi.org/10.1016/j.asr.2005.07.027

Wouters, B., Gardner, A. S., & Moholdt, G. (2019). Global glacier mass loss during the GRACE satellite mission (2002–2016). *Frontiers in Earth Science*, *7*. https://doi.org/10.3389/feart.2019.00096

Zemp, M., Huss, M., Thibert, E., Eckert, N., McNabb, R., Huber, J., et al. (2019). Global glacier mass changes and their contributions to sea-level rise from 1961 to 2016. *Nature*, *568*(7752), 382–386. https://doi.org/10.1038/s41586-019-1071-0

## References From the Supporting Information

Bhattacharya, A., Bolch, T., Mukherjee, K., King, O., Menounos, B., Kapitsa, V., et al. (2021). High Mountain Asian glacier response to climate revealed by multi-temporal satellite observations since the 1960s. *Nature Communications*, *12*(1), 4133. https://doi.org/10.1038/s41467-021-24180-y

Gray, L., Burgess, D., Copland, L., Demuth, M. N., Dunse, T., Langley, K., & Schuler, T. V. (2015). CryoSat-2 delivers monthly and inter-annual surface elevation change for Arctic ice caps. *The Cryosphere*, *9*(5), 1895–1913. https://doi.org/10.5194/tc-9-1895-2015

Gray, L., Burgess, D., Copland, L., Langley, K., Gogineni, P., Paden, J., et al. (2019). Measuring height change around the periphery of the Greenland Ice Sheet with radar altimetry. *Frontiers in Earth Science*, *7*, 146. https://doi.org/10.3389/feart.2019.00146

Howat, I. M., Porter, C., Smith, B. E., Noh, M.-J., & Morin, P. (2019). The reference elevation model of Antarctica. *The Cryosphere*, *13*(2), 665–674. https://doi.org/10.5194/tc-13-665-2019

Kääb, A., Berthier, E., Nuth, C., Gardelle, J., & Arnaud, Y. (2012). Contrasting patterns of early twenty-first-century glacier mass change in the Himalayas. *Nature*, *488*(7412), 495–498. https://doi.org/10.1038/nature11324

Kääb, A., Treichler, D., Nuth, C., & Berthier, E. (2015). Brief Communication: Contending estimates of 2003–2008 glacier mass balance over the Pamir–Karakoram–Himalaya. *The Cryosphere*, *9*(2), 557–564. https://doi.org/10.5194/tc-9-557-2015

McNabb, R., Nuth, C., Kääb, A., & Girod, L. (2019). Sensitivity of glacier volume change estimation to DEM void interpolation. *The Cryosphere*, *13*(3), 895–910. https://doi.org/10.5194/tc-13-895-2019

Minowa, M., Schaefer, M., Sugiyama, S., Sakakibara, D., & Skvarca, P. (2021). Frontal ablation and mass loss of the Patagonian icefields. *Earth and Planetary Science Letters*, *561*, 116811. https://doi.org/10.1016/j.epsl.2021.116811

Moholdt, G., Hagen, J. O., Eiken, T., & Schuler, T. V. (2010). Geometric changes and mass balance of the Austfonna ice cap, Svalbard. *The Cryosphere*, *4*(1), 21–34. https://doi.org/10.5194/tc-4-21-2010

Morris, A., Moholdt, G., & Gray, L. (2020). Spread of Svalbard glacier mass loss to Barents Sea margins revealed by CryoSat-2. *Journal of Geophysical Research: Earth Surface*, *125*(8). https://doi.org/10.1029/2019JF005357

Morris, A., Moholdt, G., Laurence, G., Schuler, T., & Eiken, T. (2022). CryoSat-2 interferometric mode calibration and validation: A case study from the Austfonna ice cap, Svalbard. *Remote Sensing of Environment*, *269*, 112805. https://doi.org/10.1016/j.rse.2021.112805

Nilsson, J., Sandberg Sørensen, L., Barletta, V. R., & Forsberg, R. (2015). Mass changes in Arctic ice caps and glaciers: Implications of regionalizing elevation changes. *The Cryosphere*, *9*(1), 139–150. https://doi.org/10.5194/tc-9-139-2015

Noël, B., van de Berg, W. J., Lhermitte, S., Wouters, B., Schaffer, N., & van den Broeke, M. R. (2018). Six decades of glacial mass loss in the Canadian Arctic Archipelago. *Journal of Geophysical Research: Earth Surface*, *123*(6), 1430–1449. https://doi.org/10.1029/2017JF004304

Noël, B., Jakobs, C. L., van Pelt, W. J. J., Lhermitte, S., Wouters, B., Kohler, J., et al. (2020). Low elevation of Svalbard glaciers drives high mass loss variability. *Nature Communications*, *11*(1), 4597. https://doi.org/10.1038/s41467-020-18356-1

Nuth, C., Moholdt, G., Kohler, J., Hagen, J. O., & Kääb, A. (2010). Svalbard glacier elevation changes and contribution to sea level rise. *Journal of Geophysical Research*, *115*(F1), F01008. https://doi.org/10.1029/2008JF001223

Pfeffer, W. T., Arendt, A. A., Bliss, A., Bolch, T., Cogley, J. G., Gardner, A. S., et al. (2014). The Randolph Glacier Inventory: A globally complete inventory of glaciers. *Journal of Glaciology*, *60*(221), 537–552. https://doi.org/10.3189/2014JoG13J176

Porter, C., Morin, P., Howat, I., Noh, M.-J., Bates, B., Peterman, K., et al. (2018). ArcticDEM. *Harvard Dataverse*. https://doi.org/10.7910/DVN/OHHUKH

Rizzoli, P., Martone, M., Gonzalez, C., Wecklich, C., Borla Tridon, D., Bräutigam, B., et al. (2017). Generation and performance assessment of the global TanDEM-X digital elevation model. *ISPRS Journal of Photogrammetry and Remote Sensing*, *132*, 119–139. https://doi.org/10.1016/j.isprsjprs.2017.08.008

Sánchez-Gámez, P., Navarro, F. J., Benham, T. J., Glazovsky, A. F., Bassford, R. P., & Dowdeswell, J. A. (2019). Intra- and inter-annual variability in dynamic discharge from the Academy of Sciences Ice Cap, Severnaya Zemlya, Russian Arctic, and its role in modulating mass balance. *Journal of Glaciology*, *65*(253), 780–797. https://doi.org/10.1017/jog.2019.58

Shean, D. E., Bhushan, S., Montesano, P., Rounce, D. R., Arendt, A., & Osmanoglu, B. (2020). A systematic, regional assessment of high mountain Asia glacier mass balance. *Frontiers in Earth Science*, *7*. https://doi.org/10.3389/feart.2019.00363

WGMS. (2021). Fluctuations of glaciers database [Dataset]. World Glacier Monitoring Service (WGMS). https://doi.org/10.5904/wgms-fog-2021-05

Zheng, W., Pritchard, M. E., Willis, M. J., & Stearns, L. A. (2019). The possible transition from glacial surge to ice stream on Vavilov Ice Cap. *Geophysical Research Letters*, *46*(23), 13892–13902. https://doi.org/10.1029/2019GL084948